ELSEVIER

Biophysical Chemistry 92 (2001) 103–117

Biophysical Chemistry

www.elsevier.com/locate/bpc

The role of facilitated diffusion in oxygen transport by cell-free hemoglobins: implications for the design of hemoglobin-based oxygen carriers

Michael R. McCarthy, Kim D. Vandegriff*, Robert M. Winslow

Departments of Bioengineering and Medicine, University of California, San Diego, CA 92161, USA

Received 10 April 2001; received in revised form 20 June 2001; accepted 21 June 2001

Abstract

We compared rates of oxygen transport in an in vitro capillary system using red blood cells (RBCs) and cell-free hemoglobins. The axial P_{O_2} drop down the capillary was calculated using finite-element analysis. RBCs, unmodified hemoglobin (HbA_0), cross-linked hemoglobin ($\alpha\alpha$-Hb) and hemoglobin conjugated to polyethylene-glycol (PEG-Hb) were evaluated. According to their fractional saturation curves, PEG-Hb showed the least desaturation down the capillary, which most closely matched the RBCs; HbA_0 and $\alpha\alpha$-Hb showed much greater desaturation. A lumped diffusion parameter, K^*, was calculated based on the Fick diffusion equation with a term for facilitated diffusion. The overall rates of oxygen transfer are consistent with hemoglobin diffusion rates according to the Stokes–Einstein Law and with previously measured blood pressure responses in rats. This study provides a conceptual framework for the design of a 'blood substitute' based on mimicking O_2 transport by RBCs to prevent autoregulatory changes in blood flow and pressure.

Keywords: Artificial capillary; Diffusive oxygen transport; Blood substitutes

1. Introduction

Solutions of cell-free hemoglobins are being designed for use as O_2-carrying resuscitation fluids to take the place of blood transfusions. However, unusual biological feedback mechanisms have been observed in animals, including man, in which the majority of these solutions cause hypertension as the result of blood vessel constriction (see [1] and references therein). The physiologic mechanism(s) governing this response may be numerous and are incompletely resolved.

A key hypothesis related to hemoglobin-induced hypertension is that acellular hemoglobins scavenge the endothelial-derived relaxing factor, nitric oxide (NO) [2], possibly due to extravasation of the cell-free hemoglobin into the interstitium between endothelial and smooth muscle cells, thereby altering the distribution of NO [3–5].

* Corresponding author. Present address: Sangart, Inc., 11189 Sorrento Valley Rd., Ste. 104, San Diego, CA 92121, USA. Tel.: +1-858-455-0966; fax: +1-858-455-6963.

E-mail address: kvandegriff@sangart.com (K.D. Vandegriff).

0301-4622/01/$ - see front matter
PII: S0301-4622(01)00194-6

In an earlier report, we demonstrated that hemoglobin-induced hypertension cannot be due solely to NO scavenging based on studies with various types of modified hemoglobins (cross-linked, polymeric or surface-conjugated), which elicited various blood pressure responses that correlated with the size of the hemoglobin molecule but not with NO reactivity [6]. Others have also shown that the size of the hemoglobin molecule [7,8], or perhaps surface modification in the case of glutaraldehyde polymerization [9], correlate with the blood pressure response, but direct measurements of extravasation of hemoglobins show that even large, surface-conjugated hemoglobins rapidly extravasate in rat mesentary [10] and in guinea pig arteries [11].

Another effect of endothelial-derived NO is the oxygen-linked *S*-nitrosylation reactions of hemoglobin, which have been shown to regulate blood flow [12,13]. The transnitrosylation reactions reported in those studies occur over a relatively slow time scale, even in the presence of low molecular weight thiols, so it is unlikely that this mechanism can explain the immediate increase in blood pressure observed with cell-free hemoglobins.

Alternatively, it has been suggested by us and by others that normal compensatory mechanisms may work to regulate O_2 delivery to tissue by cell-free oxygen carriers [14]. This hypothesis is based on the dynamic change in O_2 transfer when the O_2 carrier is a homogeneous solution of hemoglobin compared to a particulate suspension of RBCs [15–17]. Normally, the bulk of O_2 is carried in blood bound as oxyhemoglobin inside red blood cells (RBCs). Under normal physiologic conditions, when the kinetics of O_2 binding are not limiting, there is intraluminal resistance to O_2 movement out of the RBC, through the plasma, and to its site of consumption in tissue at the mitochondria. This resistance is comprised of a series of diffusion barriers: (1) the rate of O_2 diffusion out of the RBC is low because of the high concentration of intracellular hemoglobin (35 g/dl) (e.g. $D_{O_2} = 2 \times 10^{-5}$ cm^2/s in water vs. 0.75×10^{-5} cm^2/s inside RBCs [18]); (2) the solubility of O_2 in plasma is low (1.2 μM/torr [19]); (3) plasma layers immediately surrounding the RBC and at the endothelial wall do not mix with the flowing solution and create unstirred layers [20,21]; and (4) the effective capillary surface area available for O_2 diffusion in a discrete particle model, depending on hematocrit, is approximately 50% of the total capillary surface area [22].

Hellums and co-workers originally designed an in vitro artificial capillary apparatus to quantify these diffusional effects using a microscopic silicone hollow fiber mounted onto a microscope. Using tracking optics to measure hemoglobin fractional saturation as a function of flow through an environmentally-controlled chamber, they were the first to show accelerated O_2 transfer from cell-free hemoglobin solutions when compared to RBC suspensions [23,24]. An advantage of the in vitro capillary system is that O_2 transfer can be studied without the biological feedback mechanisms that regulate blood flow and vessel diameter in vivo.

In this report, we describe a simple, new system for in vitro capillary experiments that uses independently measured oxygen equilibrium curves, direct measurement of the O_2 partial pressure (PO_2) flux down the capillary tube and an algorithm to calculate the overall transfer of O_2 as a lumped diffusion parameter, K^*, based on Fick's law of diffusion [25].

Fick's law of diffusion is shown in Eq. (1). The second term in Eq. (1) indicates the contribution to total O_2 flux by the addition of freely diffusing hemoglobin (i.e. facilitated diffusion [18,26]);

$$-J = \frac{D_{O_2}\Delta[O_2]}{\Delta r} + \frac{D_{HbO_2}\Delta Y[Hb]_T}{\Delta r} \qquad (1)$$

where D_{O_2} and D_{HbO_2} are the molecular diffusion constants for O_2 and HbO_2, respectively, $\Delta[O_2]$ is the change in oxygen concentration, such that $\Delta[O_2]/\Delta r$ gives the O_2 concentration gradient, ΔY is the change in hemoglobin saturation and $[Hb]_T$ is the total cell-free hemoglobin concentration, such that $([Hb]_T \times \Delta Y)/\Delta r$ gives the HbO_2 concentration gradient. The diffusion distance, r, is considered to be from the center of the vessel wall. O_2 flux is a linear function of the oxygen concentration, whereas HbO_2 flux is a non-linear function of the oxyhemoglobin concen-

tration gradient, $\Delta Y[\mathrm{Hb}]_T/\Delta r$, based on the shape and position of the oxygen equilibrium curve (i.e. a property of the hemoglobin molecule).

In the second term of Eq. (1), the macromolecular diffusion constant (D_{HbO_2}) is defined by the Stokes–Einstein equation [27]. This equation demonstrates that the diffusion of a macromolecule is inversely proportional to the viscosity of the solution (η) and to the radius of the macromolecule (r_{ad}):

$$D_{\mathrm{HbO}_2} = \frac{kT}{6\pi\eta r_{ad}} \quad (2)$$

where k is the Boltzmann constant, and T is temperature.

The in vitro capillary hollow fiber used in these experiments is 57 μm in diameter to mimic the size of A_2/A_3 arterioles. This is relevant to studies of the microcirculation, because hemoglobin-induced vasoconstriction occurs in pre-capillary resistance arterioles, whereas capillaries are not directly subject to smooth-muscle mediated vasoactivity [28,29].

In this study, we report rates of O_2 transfer out of the in vitro capillary during constant flow using RBC suspensions and three cell-free hemoglobin solutions that vary in physical properties (size, viscosity and oxygen affinity). Our results point to effects of facilitated diffusion on rates of O_2 transfer, which are quantified by a lumped diffusion parameter, K^*. As originally reported by Hellums and co-workers, we also observe accelerated O_2 transfer with non-surface conjugated tetrameric hemoglobins when compared to RBCs. However, we show here for the first time that O_2 transfer out of an artificial capillary is not accelerated when the cell-free hemoglobin is the type of polyethylene glycol (PEG) surface-conjugated tetramer used in this experiment. This suggests that the overall rate of O_2 transfer is governed by macromolecular diffusive properties and the oxygen affinity of the acellular hemoglobin. We demonstrate that these rates of O_2 transfer correlate with previously reported data of blood pressure responses in rats following exchange transfusion with these three hemoglobin solutions [6,30]. Taken together, these results support a mechanism that links O_2 delivery to blood flow regulation.

2. Experimental methods

2.1. Test solutions

Human red blood cells (RBCs) were obtained from healthy volunteers and washed three times with normal saline to remove plasma and buffy coat components. Two 64-kD tetrameric hemoglobins were studied: (1) purified tetrameric human hemoglobin A_0 (HbA_0), provided as a gift from the US Army Blood Research Detachment, Walter Reed Army Institute for Research (Bethesda, MD) and Hemosol Inc. (Toronto, ON, Canada); (2) human tetrameric hemoglobin intramolecularly cross-linked between α Lys99 residues using a covalent chemical bridge by reaction with bis(3,5-dibromosalicyl)fumarate (αα-Hb), provided as a gift from the US Army Blood Research Detachment, Walter Reed Army Institute for Research (Bethesda, MD); and (3) a larger molecular weight tetrameric bovine hemoglobin surface-conjugated to methoxypolyethylene glycol (approx. 120 kD) (PEG-Hb) was provided as a gift from Enzon (Piscataway, NJ). The non-conjugated tetrameric hemoglobins have a molecular radius the size of native tetrameric hemoglobin (radius ~3.2 nm); the conjugated hemoglobin has a larger molecular radius of ~14 nm, due to the hydrophilic nature of polyethylene glycol, which creates a coat of water surrounding the hemoglobin protein [31]. (See Table 1 for a list of physical properties of the samples.)

Hemoglobin concentration was determined by visible spectrophotometry using a Milton Roy 3000 diode array spectrophotometer, using an extinction coefficient of 7.12 $\mathrm{mM}^{-1}\ \mathrm{cm}^{-1}$ at 523 nm [32]. Spectral analysis was performed using multicomponent analysis to determine the percentage of methemoglobin. RBC hemoglobin concentration was determined using a β-Hemoglobin Photometer (HemoCue, Angelholm, Sweden) in which the cells are introduced into a mounted cuvette where they are lysed and the hemoglobin is converted to azomethemoglobin for determination of

Table 1
Physical properties of the O_2-carrying samples

Adair constants	RBC	HbA_0	PEG-Hb	αα-Hb
a_1	1.53×10^{-2}	$4.01 \pm 0.82 \times 10^{-2}$	$1.47 \pm 0.39 \times 10^{-1}$	$2.26 \pm 0.26 \times 10^{-2}$
a_2	1.10×10^{-3}	$1.74 \pm 0.44 \times 10^{-3}$	$4.27 \pm 0.20 \times 10^{-2}$	$9.89 \pm 0.19 \times 10^{-4}$
a_3	1.24×10^{-7}	$5.95 \pm 5.95 \times 10^{-13}$	$2.46 \pm 1.91 \times 10^{-4}$	$1.67 \pm 0.69 \times 10^{-11}$
a_4	1.81×10^{-6}	$2.48 \pm 0.57 \times 10^{-5}$	$1.47 \pm 0.13 \times 10^{-4}$	$1.14 \pm 0.13 \times 10^{-6}$
P50[a]	28.6	15.1	10.2	33.1
n50[a]	2.62	2.97	1.38	2.43
Viscosity (cp)[b]	–	0.9	3.2	0.9
COP (mmHg)[b]	–	16.4	118.0	16.2
Radius (Å)	–	32[c]	141[d]	31[d]
Molecular weight (kDa)	–	64[c]	117[d]	69[d]
[Hb], g/dl	4.8	4.8	4.2	4.8

[a] *Conditions*: pH 7.4; 0.1 M Cl^-; 37°C [33].
[b] Measured at 5 g/dl.
[c] Fermi and Perutz (1984) by X-ray crystallography [50].
[d] Vandegriff et al. (1997) by thermodynamic analysis of COP; errors are ±10–15% [31].

concentration using built-in optical filters. The percent methemoglobin was less than 2–4% in every sample tested.

2.2. Oxygen equilibrium curves

Oxygen equilibrium curves for the hemoglobin samples were measured using diode array spectrophotometry with catalytic deoxygenation of oxyhemoglobin and multicomponent analysis as described previously [33]. Oxygen equilibrium curves for the RBC suspension were determined as described previously [19]. Adair constants were fitted from the measured oxygen equilibrium curve data using least-squares minimization curve fitting routines (MATLAB, The Math Works, Inc., Natick, MA) and are given in Table 1.

2.3. Artificial capillary system

A schematic diagram of the artificial capillary apparatus is shown in Fig. 1. The capillary is manufactured from highly-permeable silicone (polydimethylsiloxane Silastic, Point Medical Corporation, Crown Point, IN) using an extrusion process to produce a hollow fiber tube 57 μm in diameter. (The tube diameter is as small as can be manufactured to retain structural integrity.) Glass capillaries, made from 2-μl Microccap pipettes (Drummond Scientific, Broomall, PA), are used to connect the silicone capillary at one end to an infusion syringe pump and at the opposite end to a withdrawal syringe pump. A seal is made between the glass and silicone capillaries using General Electric RTV 60 silicone. The sample is introduced through a gas-tight syringe (Hamilton Co., Reno, NV) using an infusion pump (KD Scientific, Boston, MA). The syringe is fitted to the capillary entrance using low-permeability Tygon tubing connected through a micro-tube connector (Cole-Parmer, Niles, IL). A collection cell made of solid acrylic with a T-shaped channel (diameter 0.75-mm) is used at the exit port of the capillary. One channel is shunted through a calibrated measuring tube that serves as a flow meter. The other flow channel is directed to a gas-tight septum and the gas-tight withdrawal syringe, which is mated to the exit port using a polypropylene microfitting sealed with silicone sealant (Cole-Parmer). The needle of the syringe pierces the septum, and the sample is collected using the withdrawal pump. The rate of withdrawal is lower than the flow rate in the capillary to avoid cavitation. The entire length of the exchange chamber is approximately 25 cm.

The length of a capillary used for these experiments was 11 cm. This dimension was chosen, based on the flow rates used, because it allows

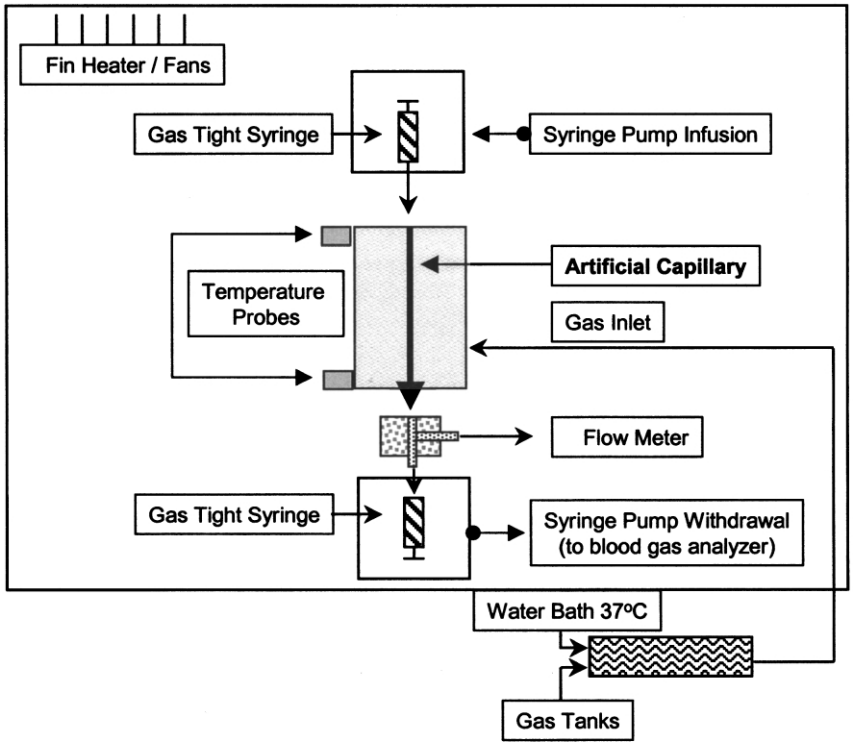

Fig. 1. Schematic diagram of the artificial capillary apparatus.

resident times similar to those observed in vivo (i.e. 0.4–1.5 s for the artificial capillary compared with 0.75 s for in vivo capillary transit [34]). The capillary is encased in a gas-tight exchange chamber made of clear acrylic plastic. The entire apparatus is enclosed within an acrylic box with a fin heater and controller for temperature control. Bimetallic temperature probes (YSI 700,Yellow Spring, OH) are attached near the entry and exit ports of the fluid flow to ensure that temperature is maintained constant at 37°C.

2.4. Capillary protocol

The necessary measurement from the capillary apparatus is the difference in P_{O_2} at the entry and exit ports of the capillary. Based on the Adair constants fitted to the oxygen equilibrium curve data (see above), calculations are made of the amount of O_2 transferred out of the capillary by radial diffusion as the sample flows down the axial length of the gas-exchange chamber.

Test solutions were diluted to similar concentration (4.2–4.8 g/dl) and equilibrated with humidified air in an IL 2000 tonometer (Instrumentation Laboratories, Lexington, MA). The equilibrated samples were transferred in a gas-tight syringe to the infusion pump. Flow was established throughout the system at a selected flow rate: 10; 20; or 40 μl/min, giving capillary resident times of 1.56, 0.75 and 0.39 s, respectively.

Each test solution was first pumped through the capillary in an air-equilibrated environment to verify no change in P_{O_2} at the entry and exit ports. The gas environment outside of the capillary was then switched to pure N_2, humidified at 37°C, at constant flow to replace the volume of gas in the exchange chamber every 10 s. Clark-type oxygen electrodes (Instech, Plymouth Meeting, PA) were used to check the gas composition in the exchange chamber: over 95% of O_2 was removed from the chamber within 1 min; and zero O_2 was detected in the chamber after 2 min. A

5-min delay period from the beginning of chamber gas flow to the start of sample collection was allowed to insure 100% gas exchange and to purge residual fluid in the collection cell.

Samples from the gas-tight syringes at the entry and exit ports were analyzed using a Radiometer ABL-5 blood gas analyzer (West lake, Ohio) for measurements of P_{O_2} and pH. Each P_{O_2} data point represents a minimum of three measurements with an overall error of approximately ± 3 mmHg. The overall error was determined by the error inherent to the blood gas analyzer measurement (~ 1.5 mmHg) and the range in the data from triplicate experiments (~ 1–2 mmHg).

2.5. Experimental premise and assumptions

The premise of the experiment is that if we know the precise oxygen equilibrium curve of the oxygen carrier, the length of the capillary, the diameter of the capillary, the flow rate, the P_{O_2} outside the capillary and the starting P_{O_2} inside the capillary and if we assume that all O_2 compartments are in chemical equilibrium, the oxygen equilibrium curve of the sample does not change in the capillary, transport of O_2 out of the capillary is governed by Fick's law of diffusion, that permeability of the capillary material is not rate limiting and that the system behaves like a series of small diffusion chambers without effects from streaming, flowing or other effects, we then measure the P_{O_2} at the exit of the capillary. Now, using the finite-element technique (see below), we can model the movement of O_2 through its various compartments in each element until the exit P_{O_2} equals that actually measured. We find we must introduce a new parameter, K^*, which acts like a diffusion parameter based on the diffusion constants in the Fick equation [Eq. (1)], and is unique for each solution.

2.6. Calculations

A FORTRAN program was derived to model the loss of O_2 during the transit of the sample down the capillary. The calculation uses a finite-element analysis such that the amount of O_2 transferred out at each finite-element segment ($\Delta x = 1$ mm) (see Fig. 2) was calculated based on the hemoglobin concentration and oxygen equilibrium curve for each sample. The finite-element iterative method has been used for mathematical modeling of hemoglobin reactions (see [35] and references therein) and is described in detail for our application as follows: for each finite-element axial segment (Δx) along the capillary, the total O_2 present in solution is:

$$O_{2_T} = \alpha P_{O_2} + Y[\mathrm{Hb}]_T \tag{3}$$

where α is the solubility coefficient of O_2 in plasma (1.2074 μM/torr) [19], P_{O_2} is the partial pressure of O_2, Y is the fractional saturation of hemoglobin with O_2 and $[\mathrm{Hb}]_T$ is total hemoglobin concentration. The amount of O_2 transferred out of the capillary is calculated in each axial segment (Δx) as:

$$\Delta O_2 = \frac{K^*(\Delta P_{O_2})(\pi r^2)\Delta x}{R} \tag{4}$$

where ΔO_2 is the O_2 loss along each axial Δx segment, K^* is a lumped diffusion parameter in units of μM min^{-1} torr^{-1}, consisting in part of the diffusion constants in Eq. (1), ΔP_{O_2} is the radial O_2 gradient [i.e. P_{O_2} (inside) $- P_{O_2}$ (outside)] (this number is assumed to equal the P_{O_2} (inside), because P_{O_2} (outside) is maintained at zero in the constant flow of pure N_2 gas surrounding the capillary), r is the radius of the capillary, Δx is the axial segment of the capillary used for the finite-element analysis (i.e. 1 mm) and R is the flow rate in ml/min.

The total O_2 (O_{2T}) Eq. (3) in each axial segment, Δx, is then decremented by ΔO_2 Eq. (4), and P_{O_2} and Y values are calculated in increments of $P_{O_2} = 1$ torr from Adair parameters (see Table 1). The mathematical program then tests each (P_{O_2}, Y) pair until the appropriate combination is found that provides the new value of O_{2T}. This process is repeated for each Δx increment until the end of the capillary is reached. The end-capillary P_{O_2} is compared to the measured value at the capillary exit port, and the program reiterates after adjusting the value of K^* until the measured and fitted values for P_{O_2} agree to within 1 torr.

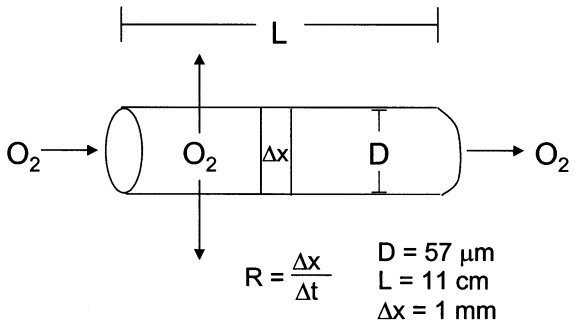

Fig. 2. Diagram of the finite-element mathematical model (not drawn to scale). Oxygen enters the vessel segment by convection and escapes by both convection and diffusion (shown by arrows). D, diameter of the hollow fiber capillary (57 μm); L, length of capillary (11 cm); Δx, finite element capillary segment (1 mm); and R = flow rate.

3. Results

The diffusion constants for O_2 (D_{O_2}) and for tetrameric HbO_2 (D_{HbO_2}) (at the hemoglobin concentration used in these experiments, ~3 mM in heme) are given in Table 2. D_{HbO_2} ($\sim 1 \times 10^{-6}$ cm^2/s) is approximately 1/20th of D_{O_2} ($\sim 2 \times 10^{-5}$ cm^2/s). However, because of the low solubility of O_2 in plasma ($\alpha = 1.2074$ μM/torr), the concentration of O_2 at a P_{O_2} of 100 torr is only 0.12 mM. Therefore, the overall amount of O_2 transferred, calculated as the diffusion constant × the concentration of diffusing molecule (i.e. either O_2 or HbO_2), is effectively doubled in the presence of 3-mM hemoglobin.

Fig. 3 shows capillary exit P_{O_2} values as a function of residence time for each sample. Theoretically, as flow reaches infinitely high rates (i.e residence time → 0), the exit P_{O_2} will be the same as the entrance P_{O_2} (i.e. air pressure ≈ 150 mmHg). Conversely, as flow stops (i.e. residence time → ∞), the samples would have time to desaturate completely, and the exit P_{O_2} would be zero (data not shown). Intermediate flow rates were chosen for these experiments to mimic physiologic relevant resident times (40, 20 and 10 μl/min = residence times 0.39, 0.75 and 1.56 s, respectively). As seen in Fig. 3, the exit P_{O_2}'s were in the order of: RBC ≈ αα-Hb > PEG-Hb ≈ HbA_0. (Exact values are given in Table 3.) The ranking is consistent with the samples' oxygen affinity: RBCs and αα-Hb have relatively low oxygen affinity (P50 = 29 and 33 torr, respectively) compared to HbA_0 and PEG-Hb (P50 = 15 and 10 torr, respectively) (see Table 1). The oxygen affinity, in turn, defines the amount of oxyhemoglobin in equilibrium with the P_{O_2} of the solution.

The oxygen equilibrium curves for each sample were measured independently and are shown in Fig. 4. The filled symbols show fractional saturation values calculated at the measured exit P_{O_2} values. Thus, even though RBCs (○) and αα-Hb (◇) have similar oxygen equilibrium curves they desaturate at very different rates: αα-Hb desaturates to a much greater degree compared to RBCs, particularly as residence time increases; the same is true for HbA_0 compared to PEG-Hb. The reason for the increased desaturation, particularly for αα-Hb vs. RBCs, which have very similar oxygen equilibrium curves, must be accelerated diffusion of O_2 out of the capillary from the αα-Hb solution. The actual values for exit fractional saturations as a functional of residence time are plotted in the inset to Fig. 4. The non-

Table 2
Comparison of passive and facilitated O_2 diffusion at $P_{O_2} = 100$ torr

	Concentration (mM)	Diffusion constant (cm^2/s)[a]	Flow transfer = (concentration × diffusion) ($mM \cdot cm^2/s$)
@P_{O_2} 100 torr			
O_2	0.12074	1.96×10^{-5}	2.37×10^{-6}
HbO_2	3.0	9.70×10^{-7}	2.91×10^{-6}

[a]Average value based on the measured values from Wittenberg (1970) and Kreuzer (1970) [26,18] adjusted to temperature 37°C based on estimated temperature effects on the diffusion constant for myoglobin [51].

Table 3
Capillary oxygenation parameters of the solutions used in the experiments

Flow (μl/min)	Residence time (s)	P_{O_2} (mmHg)	K^* (μM/min·mmHg)	Saturation (fraction)
RBC				
0	0	159	–	0.986
40	0.39	53	1086	0.836
20	0.75	42	1032	0.735
10	1.56	34	877	0.612
HbA_0				
0	0	151	–	0.990
40	0.39	25	2564	0.820
20	0.75	17	3838	0.586
10	1.56	11	4301	0.287
αα-Hb				
0	0	152	–	0.998
40	0.39	51	1591	0.747
20	0.75	36	1826	0.551
10	1.56	24	1772	0.321
PEG-Hb				
0	0	158	–	0.998
40	0.39	34	1076	0.878
20	0.75	24	1120	0.794
10	1.56	16	1209	0.660

conjugated tetrameric hemoglobins (αα-Hb and HbA_0) show similar, highly desaturating profiles over time. In contrast, RBCs and PEG-Hb show similar, less desaturing profiles over time, even though PEG-Hb is an acellular solution. Oxygen affinity defines the amount of oxyhemoglobin in equilibrium with the P_{O_2} of the solution, which is a function of the shape and position of the oxygen dissociation curve. Based on the fractional saturation curve, the oxyhemoglobin concentration gradient is dependent on how much O_2 dissociates from the hemoglobin at a given P_{O_2}. If the hemoglobin remains highly saturated, such as with the PEG-Hb, its facilitated diffusion is limited because its concentration gradient is shallow.

The experimentally determined diffusion parameters, K^*, [see Eq. (4)] from the finite-element analysis are shown in Fig. 5 as a function of residence time. K^* is expected to be greater for the freely diffusing hemoglobins compared to RBCs due to the absence of the numerous intraluminal diffusion barriers for RBCs and the additional O_2 flux by facilitated diffusion [see Section 1 and the second term in Eq. (1)]. Fig. 5a shows the calculated values in units of μM min^{-1} $torr^{-1}$ (exact values are given in Table 3), such that, $HbA_0 >$ αα-Hb > PEG-Hb ≈ RBCs. When the exit P_{O_2} is taken into account to calculate K^* in units of μM/min, the rate of diffusion changes order: αα-Hb ≥ HbA_0 > RBCs > PEG-Hb (Fig. 5b). As a result, K^* for αα-Hb increases because of the higher P_{O_2} values at which αα-Hb desaturates, thus increasing the facilitated O_2 transport relative to the higher-affinity HbA_0. Interestingly, the PEG-Hb solution does not show any facilitated-diffusion effect in Fig. 5a and actually exhibits a lower diffusivity compared to RBCs in Fig. 5b, perhaps due to PEG-Hb's high O_2 affinity.

Fig. 6 shows the extrapolation of K^* values to converge at a limiting value of ~1000 μM min^{-1} $torr^{-1}$ at 0.085 s. $K^* \times$ the convergence time (in minutes) gives an O_2 concentration of 1.4 μM/torr, which equals the concentration of O_2

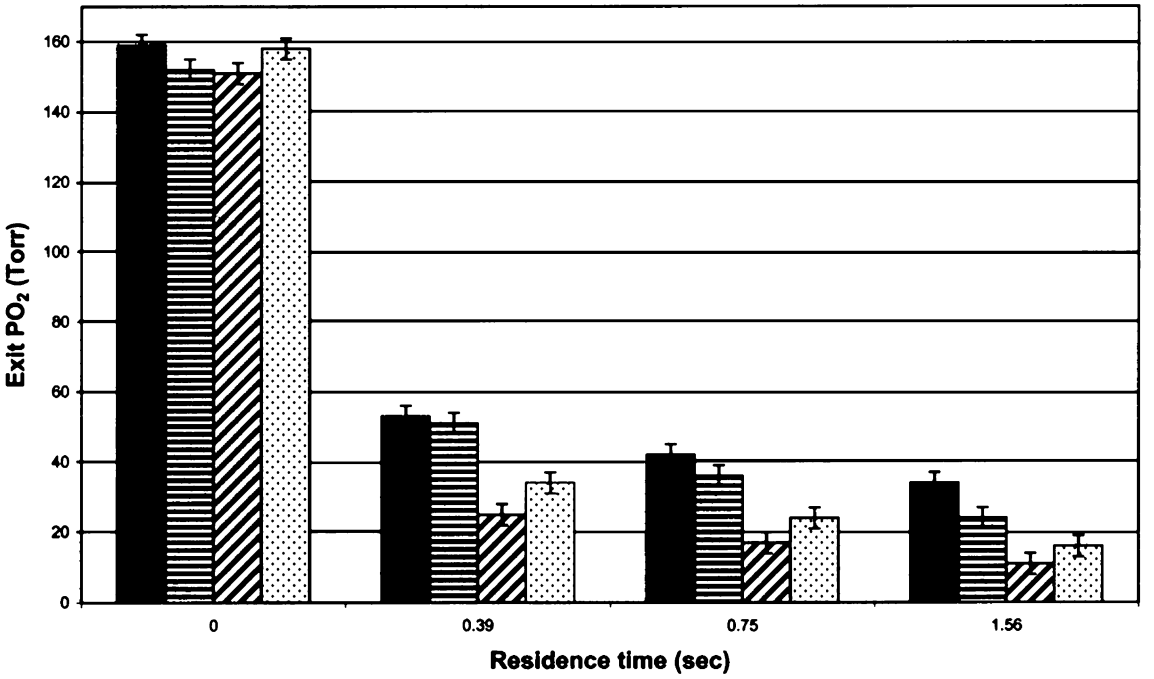

Fig. 3. PO_2 measurements as a function of residence time in the artificial capillary. Samples are taken from the exit port of the apparatus shown in Fig. 1, and PO_2 was measured in the blood gas analyzer. Legend: (■) RBCs; (▤) $\alpha\alpha$-Hb; (▨) HbA_0; (▦) PEG-Hb.

in air-saturated water at 37°C according to Henry's Law and suggests a maximum flow rate for these experiments of ~ 200 μl/min. In other words, at this rate of flow, convection would be too fast to allow loss of O_2 by radial diffusion out of the capillary.

Fig. 7 shows progress curves for the cumulative transfer of O_2 along the axial position of the capillary at each experimental flow rate. This analysis provides a ranking for the total amount of O_2 delivered from the individual samples: at the lower flow rates 10 and 20 μl/min $\alpha\alpha$-Hb $\geq$ $HbA_0 \gg$ RBCs > PEG-Hb; and at the fastest flow rate (40 μl/min), HbA_0 > Hb > RBCs > PEG-Hb.

4. Discussion

Hemoglobin-based blood substitutes are being designed to reduce the need for blood transfusions. They would eliminate infectious transmission of blood-borne diseases and avoid the rising costs of blood collection and testing. The oxygen-carrying capacity of hemoglobin has made it an obvious choice for such a product. Cross-linking the hemoglobin tetramer either chemically or genetically, polymerizing hemoglobin molecules to make oligomers or attaching hydrophilic polymers to the surface of hemoglobin have all been successful at preventing pathological hemoglobinuria. Even so, these first-generation products have progressed slowly [1,36]. Resolution of the mechanism of hemoglobin-induced vasoconstriction is the central issue facing development of red cell substitutes.

Amberson realized as early as 1949 that cell-free hemoglobin solutions were vasoactive [37]. He noted that his patients became hypertensive when they received stroma-free hemoglobin. Later studies in the isolated, perfused heart model showed that hemoglobin-induced vasoconstriction is a result of interaction of hemoglobin with the

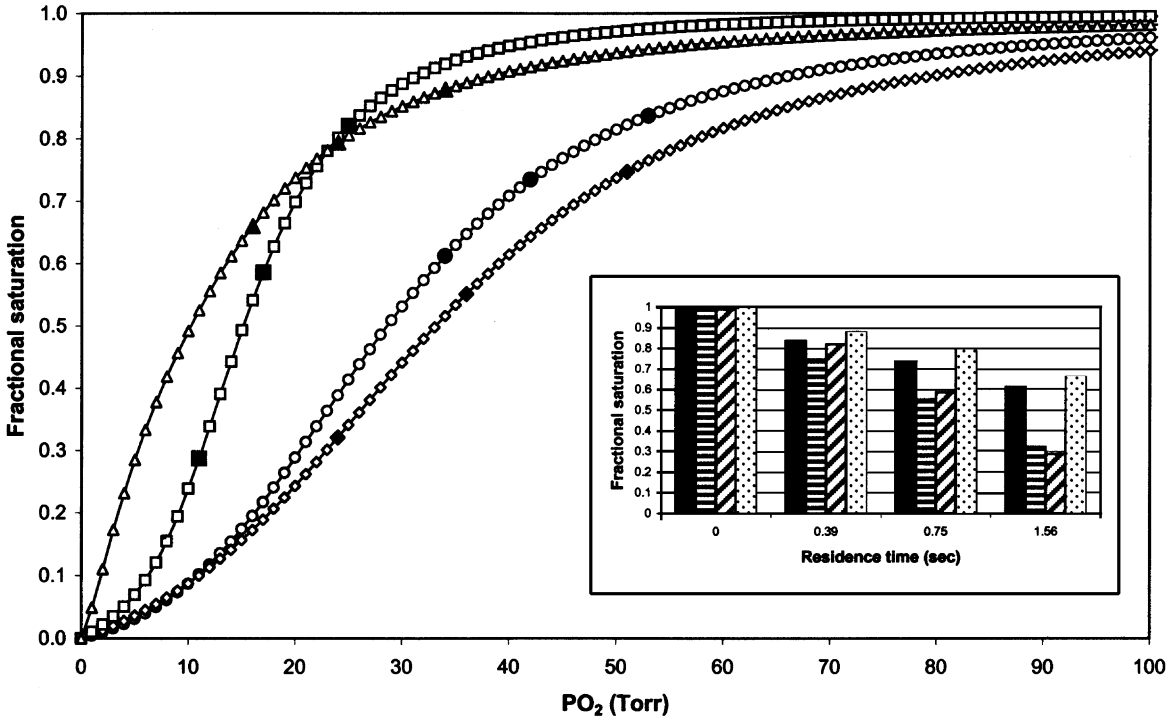

Fig. 4. Oxygen equilibrium curves. Experimental conditions: 0.1 M Cl^-, pH 7.4, 37°C. Symbols show data points: (○) RBCs; (◇) αα-Hb; (□) HbA_0; (△) PEG-Hb. The curves are presented from calculations using fitted Adair constants listed in Table 1. The corresponding P50 and Hill coefficients (n50) are also given in Table 1. The fractional saturation corresponding to each capillary exit PO_2 value at the different flow rates are shown by the filled symbols. Fig. 4 (inset) shows the fractional saturation determined from the exit PO_2 as a function of capillary residence time: Legend: (■) RBCs; (▤) αα-Hb; (▨) HbA_0; (▦) PEG-Hb.

vasculature itself, rather than a more general neurally-mediated mechanism [38,39]. More recently, direct observations in the microcirculation have shown that some hemoglobin solutions cause a narrowing of A_2/A_3 arterioles, restricting blood flow to the capillaries [40].

The practical problem of hemoglobin-induced vasoconstriction is illustrated by a study done by the US Army to evaluate hemoglobin solutions for the battlefield. Pigs were dehydrated to simulate battlefield conditions and then subjected to a controlled hemorrhage [41]. They were resuscitated with either the non-oxygen carrier albumin, or cell-free oxygen carriers HbA_0 or αα-Hb and hemodynamic and oxygen transport measurements were made. Both hemoglobin solutions caused an immediate increase in the animals' blood pressure. These studies showed that in spite of increased O_2 carrying capacity conferred by the hemoglobin solutions, O_2 delivery was the same as with the albumin solution. The rise in blood pressure and fall in cardiac output offset any advantage of administration of the hemoglobin solutions. These studies established a link between vasoconstriction and O_2 transport.

The mammalian circulation is tightly balanced to match O_2 delivery to local O_2 demand [42]. The control mechanism is a complicated series of multiple feedback loops, including interrelated functions of blood flow, blood vessel diameter and endothelial shear stress to maintain adequate oxygen tension at the tissue level. Control is achieved through dynamic adjustment of vascular smooth muscle tension by vasoconstriction or vasodilation, depending on metabolic need [43]. Mounting evidence suggests that a flavoheme protein, universally present in all cells, acts as an oxygen sensor through a signal transduction path-

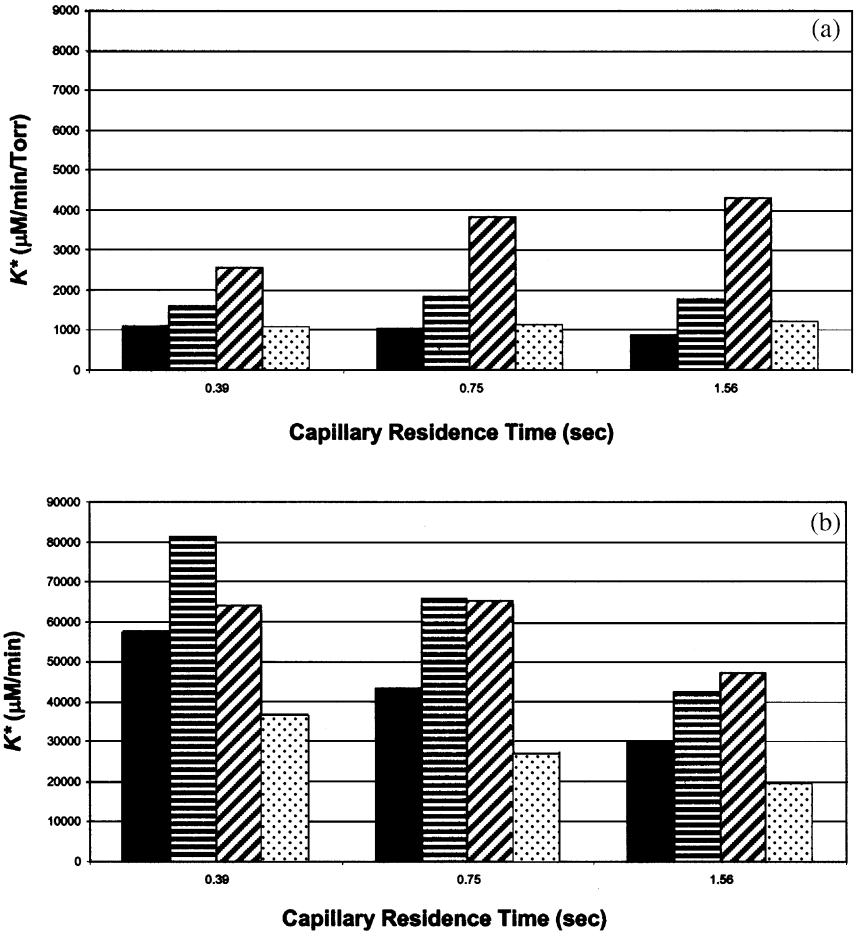

Fig. 5. (a) Calculated lumped diffusion constants (K^*, μM/min/Torr, see Eq. (4)) as a function of capillary residence time in the artifical capillary. (b) Calculated lumped diffusion constants using exit PO_2 (K^*, μM/min, see Eq. (4)) as a function of capillary residence time: Legend: (■) RBCs; (▤) αα-Hb; (▨) HbA_0; (▦) PEG-Hb.

way that is regulated by intracellular levels of reactive oxygen intermediates [44–46]. Such regulation by an O_2 sensor is consistent with physiologic experiments showing that P_{O_2} regulates blood flow; increases in microvascular P_{O_2} decrease the production of endothelial vasodilators and provokes vasoconstriction [47,48]; high P_{O_2} reduces the number of flowing capillaries and increases resistance to blood flow [49].

The effects on blood pressure following 50% exchange transfusion in rats with the three hemoglobin samples studied here have been reported previously (see Fig. 8) [6,30]. Exchange transfusion with either αα-Hb or HbA_0 caused a significant and persistent increase in mean arterial pressure, while animal exchange transfused with PEG-Hb elicited no blood pressure response. The hypothesis for O_2-sensing autoregulatory control of blood flow in the presence of cell-free hemoglobin is consistent with the results presented here. The rate of O_2 transfer out of the in vitro microvessel (the size of resistance arterioles but devoid of biologic feedback mechanisms) correlates with observed hypertensive responses measured in vivo in which biologic feedback systems are present: i.e. αα-Hb $\geq$ HbA_0 $\gg$ PEG-Hb. The PEG-Hb solution exhibits significantly attenuated movement of O_2 out of the capillary compared to

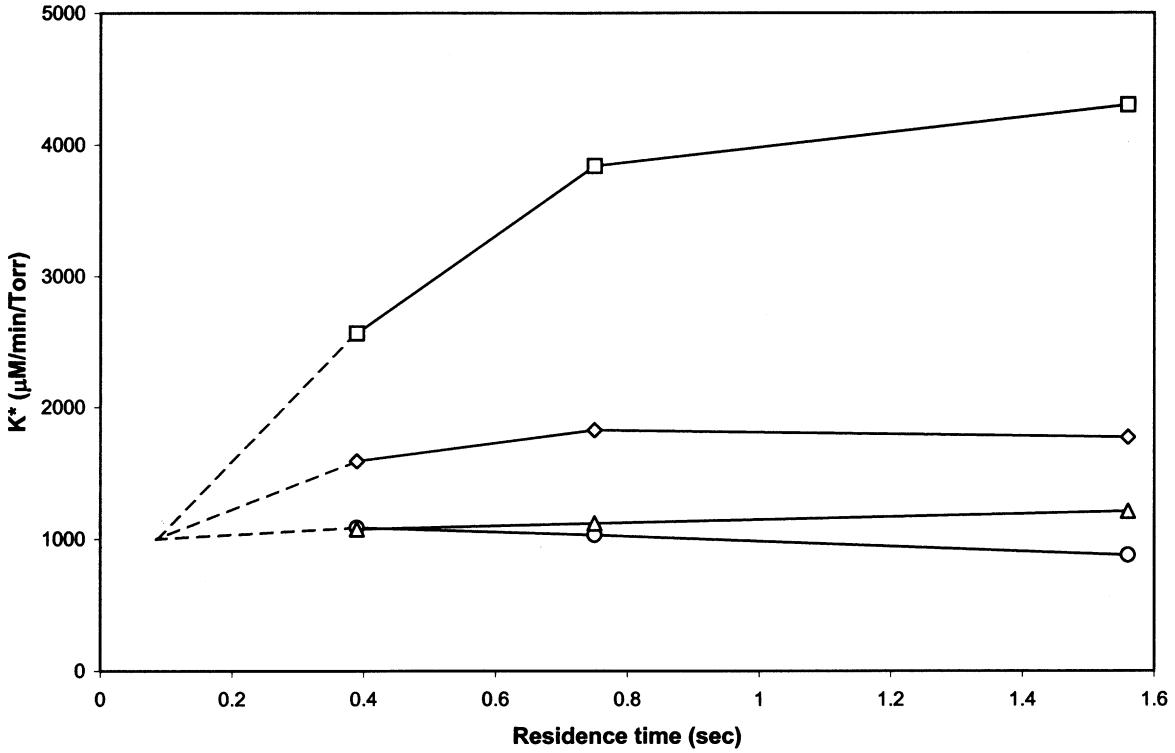

Fig. 6. Extrapolation of K^* to a limiting value for capillary residence time (0.085 s). Using this value for limiting residence time, K^* is calculated to be 1.4 μM/Torr, i.e., the concentration of O_2 in air-saturated water at 37°C based on Henry's Law constant.

αα-Hb and HbA_0 and, as a result, O_2 is transferred at a rate more similar to that for RBCs.

The Stokes–Einstein Law Eq. (2) provides a conceptual framework for strategies to limit facilitated diffusion by cell-free hemoglobins to avoid autoregulatory vasoconstriction. Macromolecular diffusivity is: (1) inversely proportional to solution viscosity (η); (2) inversely proportional to molecular size (r_{ad}); (3) directly proportional to $[Hb]_T$; and (4) directly proportional to ΔY. ΔY is a non-linear function of the co-operativity of O_2 binding, represented by the Hill coefficient (n50). ΔY is not necessarily related to the position of the equilibrium curve (i.e. P50), because the slope is determined by the shape rather than the position of the curve at a given ΔP_{O_2}.

Future experiments are planned to evaluate the effects from the individual terms in Eq. (1) that cannot be distinguished by the lumped parameter, K^*, calculated here by finite-element analysis. However, if one assumes that the diffusion constant for free O_2 does not change in the system, differences in K^* are attributed to ΔP_{O_2} and the second 'facilitated diffusion' term in Eq. (1), which is determined by the macromolecular diffusion constant and the oxygen affinity of the hemoglobin. Future experiments also are planned for this in vitro capillary system to study the O_2 transfer characteristics with combinations of RBCs and cell-free hemoglobins. Page et al. [24] showed enhanced O_2 release, relative to RBCs alone, even at a ratio of 9:1 RBCs to extracellular bovine hemoglobin solution with similar P50s (27 vs. 25 mmHg). We will explore mixtures of RBCs and PEG surface-conjugate hemoglobin to discover the limit to which RBC hematocrit can be reduced while maintaining a normal rate of O_2 transfer in the presence of extracellular hemo-

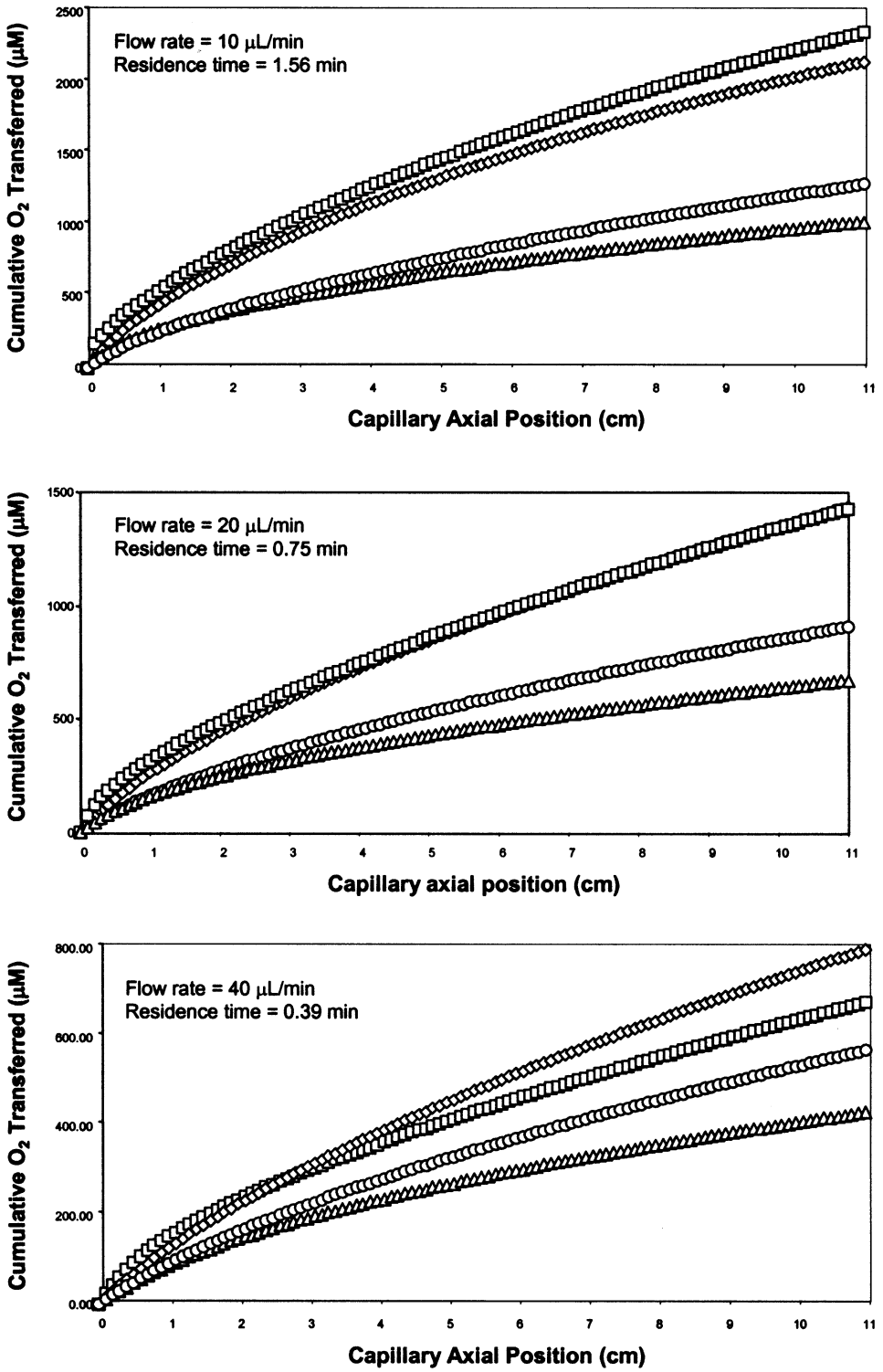

Fig. 7. Cumulative oxygen transferred out of the artificial capillary at different flow rates as a function of capillary axial position. Calculations are described in the text. Symbols: (○) RBCs; (◇) αα-Hb; (□) HbA_0; (△) PEG-Hb.

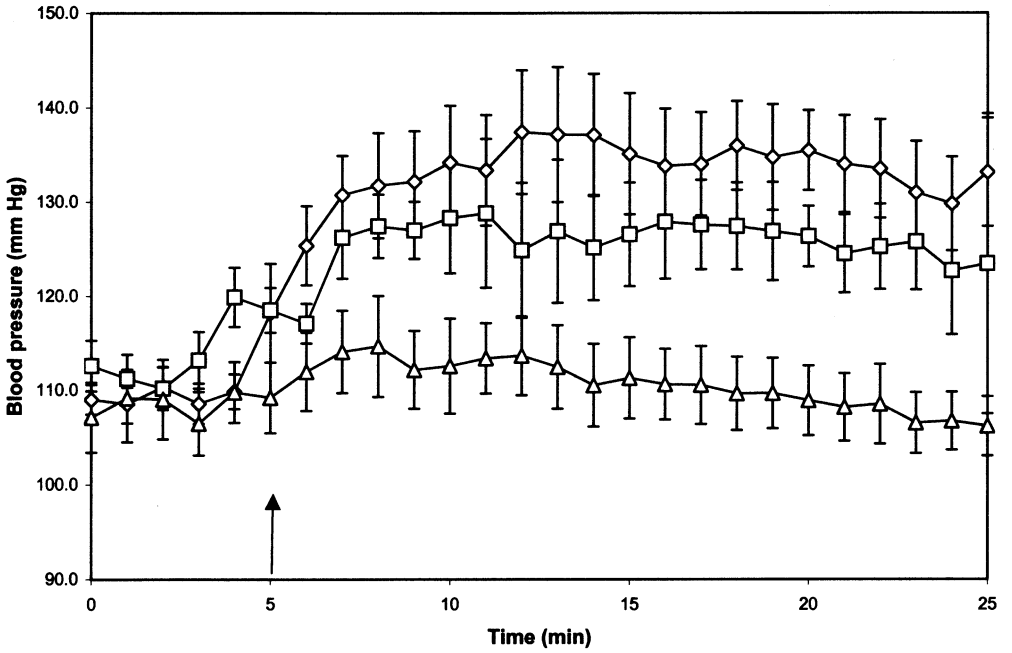

Fig. 8. Mean arterial pressures measured in rats during and after 50% exchange transfusion infusion at a rate of 0.5 ml/min with cell-free hemoglobins. Baseline blood pressure is collected for approximately 30 minutes; only the last 5 minutes are shown here. The exchange transfusion starts at the point (shown by arrow) and data were collected for 2 h post exchange; only the initial 20 min post exchange are shown here. Data are shown as means ± standard errors. Symbols (◇) αα-Hb ($n = 6$) (□) HbA_0 ($n = 4$); (△) PEG-Hb ($n = 5$). Data reproduced from [6].

globin. These experiments will determine the efficacy of PEG-hemoglobin solutions as a 'red cell substitute'.

5. Conclusion

The data presented here suggest that the typical vasoconstriction induced by hemoglobin-based blood substitutes is at least partially due to over-oxygenation of tissue by the cell-free solutions, eliciting an O_2-sensitive feedback mechanism to reduce blood flow. To avoid this counterproductive control mechanism, the rate of O_2 transfer by RBCs under normal conditions should be mimicked, which can be accomplished by limiting the facilitated diffusion of O_2 as oxyhemoglobin. The intraluminal resistance to O_2 diffusion in a hemoglobin solution does not have to be of the same nature as RBCs, but it should be of the same magnitude. Correlations between in vitro and in vivo data are necessarily circumstantial, nevertheless, our data show a correlation between the blood pressure response in rats following exchange transfusion and the diffusion of O_2 from hemoglobin solutions. HbA_0 and αα-Hb have high diffusion parameters and cause significant increases in mean arterial blood pressure. In contrast, PEG-Hb does not facilitate O_2 diffusion and, in turn, elicits no effect on blood pressure. It should now be possible to design a 'blood substitute' that does not induce autoregulatory vasoconstriction and thus maintains tissue blood flow and O_2 perfusion.

Acknowledgements

This work was supported by grants from the NIH, National Heart, Lung and Blood Institute HL48018 and HL63577.

References

[1] R.M. Winslow, Ann. Rev. Med. 50 (1999) 337.
[2] M.P. Doyle, A.M. Armstrong, E.A. Brucker, T.J. Fattor, D.D. Lemon, Artif. Cells Blood Sub. Immobil. Biotech. 29 (2001) 100.
[3] K. Nakai, T. Ohta, I. Sakuma et al., J. Cardiovasc. Physiol. 28 (1996) 115.
[4] J. Loscalzo, J. Lab. Clin. Med. 129 (1997) 580.
[5] D.H. Doherty, M.P. Doyle et al., Nat. Biotech. 16 (1998) 672.
[6] R.J. Rohlfs, E. Bruner, A. Chiu et al., J. Biol. Chem. 273 (1998) 12128.
[7] Z. Abassi, S. Kotob, F. Pieruzzi et al., J. Lab. Clin. Med. 129 (1997) 603.
[8] H. Sakai, H. Hara, M. Yuasa et al., Am. J. Physiol. 279 (2000) H908.
[9] M.P. Doyle, I. Apostol, B.A. Kerwin, J. Biol. Chem. 274 (1999) 2583.
[10] A.L. Baldwin, Am. J. Physiol. 277 (1999) H650.
[11] B. Faivre-Fiorina, A. Caron, C. Fassot et al., Am. J. Physiol. 276 (1999) H770.
[12] L. Jia, C. Bonaventura, J. Bonaventura, J.S. Stamler, Nature 380 (1996) 221.
[13] J.S. Stamler, L. Jia, J.P. Eu et al., Science 276 (1997) 2034.
[14] M. Intaglietta, P.C. Johnson, R.M. Winslow, Cardiovas. Res. 32 (1996) 632.
[15] L.D. Homer, P.K. Weathersby, L.A. Kiesow, Microvasc. Res. 22 (1981) 308.
[16] W. Federspiel, A. Popel, Microvasc. Res. 32 (1986) 164.
[17] K.D. Vandegriff, R.M. Winslow, in: R.M. Winslow, K.D. Vandegriff, M. Intaglietta (Eds.), Blood Substitutes: Physiological Basis of Efficacy, Birkhäuser, Boston, 1995, p. 143.
[18] F. Kreuzer, Respir. Physiol. 9 (1970) 1.
[19] R.M. Winslow, M.L. Swenberg, R.L. Berger et al., J. Biol. Chem. 252 (1977) 2331.
[20] K.D. Vandegriff, J.S. Olson, J. Biol. Chem. 259 (1984) 12609.
[21] J.D. Hellums, P.K. Nair, N.S. Huang, N. Ohshima, Ann. Biomed. Eng. 24 (1996) 1.
[22] J.D. Hellums, Microvasc. Res. 13 (1977) 131.
[23] D.D. Lemon, P.K. Nair, E.J. Boland, J.S. Olson, J.D. Hellums, J. Appl. Physiol. 62 (1987) 798.
[24] T.C. Page, W.R. Light, C.B. McKay, J.D. Hellums, Microvasc. Res. 55 (1998) 54.
[25] M. McCarthy, Ph.D. Thesis, University of California, San Diego, 1997.
[26] J.B. Wittenberg, Physiol. Rev. 50 (1970) 559.
[27] P. Atkins, Physical Chemistry, W.H. Freeman and Co, San Francisco, 1978.
[28] A. Tsai, H. Kerger, M. Intaglietta, in: R.M. Winslow, K.D. Vandegriff, M. Intaglietta (Eds.), Blood Substitutes: Physiological Basis of Efficacy, Birkhäuser, Boston, 1995, p. 155.
[29] A. Tsai, H. Kerger, M. Intaglietta, in: R.M. Winslow, K.D. Vandegriff, M. Intaglietta (Eds.), Blood Substitutes: New Challenges, Birkhäuser, Boston, 1996, p. 124.
[30] R.M. Winslow, A. Gonzales, M.L. Gonzales et al., J. Appl. Physiol. 85 (1998) 993.
[31] K.D. Vandegriff, M. McCarthy, R.J. Rohlfs, R.M. Winslow, Biophys. Chem. 69 (1997) 23.
[32] S.M. Snell, M.A. Marini, J. Biochem. Biophys. Meth. 17 (1988) 25.
[33] K.D. Vandegriff, R.J. Rohlfs, M.D. Magde, R.M. Winslow, Anal. Biochem. 256 (1998) 107.
[34] F.J.W. Roughton, R.E. Forster, J. Appl. Physiol. 11 (1957) 290.
[35] R.L. Berger, N. Davids, M. Perrella, Meth. Enzymol. 232 (1994) 517.
[36] K.D. Vandegriff, Exp. Opin. Invest. Drugs 9 (2000) 1967.
[37] W.R. Amberson, J.J. Jennings, C.M. Rhode, J. Appl. Physiol. 1 (1949) 469.
[38] V.W. Macdonald, in: G. Brewer (Ed.), The Red Cell. Seventh Ann Arbor Conference, Alan R. Liss, New York, 1989, p. 423.
[39] W.M. Vogel, W. Lieberthal, C.S. Apstein, N.G. Levinsky, C.R. Valeri, Biomat. Artif. Cells Artif. Org. 16 (1988) 227.
[40] H. Kerger, A.G. Tsai, D.J. Saltzman, R.M. Winslow, M. Intaglietta, Am. J. Physiol. 272 (1997) H525.
[41] J.R. Hess, V.W. Macdonald, W.W. Brinkley, J. Appl. Physiol. 74 (1993) 1769.
[42] K.N. Richmond, R.D. Shonat, R.M. Lynch, P.C. Johnson, Am. J. Physiol. 277 (1999) H1831.
[43] P.C. Johnson, K. Richmond, R.D. Shonat et al., in: R.M. Winslow, K.D. Vandegriff, M. Intaglietta (Eds.), Blood Substitutes: Physiological Basis of Efficacy, Birkhäuser, Boston, 1995, p. 175.
[44] H. Bunn, J. Gu, L. Huang, J. Park, H. Zhu, J. Exp. Biol. 201 (1998) 1197.
[45] L. Huang, J. Gu, M. Schau, H. Bunn, Proc. Natl. Acad. Sci. USA 95 (1998) 7987.
[46] H. Zhu, H. Bunn, Respir. Physiol. 115 (1999) 239.
[47] E.J. Messina, D. Sun, A. Koller, M.S. Wolin, G. Kaley, Microvasc. Res. 48 (1994) 151.
[48] A.R. Pries, J. Heide, K. Ley, K.F. Klotz, P. Gaehtgens, Microvasc. Res. 49 (1995) 289.
[49] L. Lindbom, R.F. Tuma, K.E. Arfors, Microvasc. Res. 19 (1980) 197.
[50] G. Fermi, M.F. Perutz, B. Shaanan, R. Fourme, J. Mol. Biol. 175 (1984) 159.
[51] W. Moll, Pflugers Arch. 299 (1968) 247.